A Theoretical Study of Crystallochromy. Quantum Interference Effects in the Spectra of Perylene Pigments

Peter M. Kazmaier*,† and Roald Hoffmann‡

Contribution from the Xerox Research Centre of Canada, 2660 Speakman Drive, Mississauga, Ontario, Canada L5K 2L1, and Department of Chemistry and Materials Science Center, Cornell University, Ithaca, New York 14853

Received March 2, 1994®

Abstract: The crystallochromy of perylene pigments has been explored using tight-binding extended Hückel calculations on a one-dimensional infinite stack of perylenes as a function of transverse and longitudinal offset. Although the smallest band gap occurs for perylenes when the molecules are completely eclipsed in the solid state, the general perception in the literature that the degree of "area overlap" of successive perylenes in the solid state determines simply the shift of the absorption maximum is not supported by the calculations. The nodal character of the HOMO and LUMO wave functions may be such that the area overlap is large, but the band gap and band broadening is small. This is a quantum interference effect. Calculations on one-dimensional stacks of perylenes of known structure can reproduce the trend both in the wavelength of the absorption maximum and the change in width of the absorption. An analysis of the relationship of band broadening to the photogeneration efficiencies of pigments in photoconductors shows that pigments with substantial band broadening by aggregation are precisely those which benefit most significantly by separating the hole and electron on excitation. Examples of band-broadened pigments with high photogenerating efficiencies are taken from perylenes, squaraines, thiopyrylium, and diketopyrrole photogenerators.

Introduction

Since Perkin discovered the dye mauveine in 1856, the development of color and the understanding of its origin has played a significant role in the development of chemistry.[1] The detailed understanding of the relationship of color to molecular structure has focused primarily on the role of the chromophore in determining color while much less attention has been devoted to the role of crystal packing.

This prejudice for a molecular explanation is understandable since in many cases the color of a compound can be completely interpreted by looking only at molecular (in contrast to aggregate or lattice) effects.[2] If the spectrum of a molecule does not differ much between gas, liquid, solution, and solid phases, one naturally turns to a characteristic of the individual molecule. A major exception to this trend occurs in the photographic industry, where a substantial effort has been devoted to understanding the aggregation of sensitizing dyes and to the development of laser dyes.[3]

In the areas of photographic sensitizers and laser dyes, the aggregation process primarily affects performance through a change in the absorption spectrum induced by aggregation.[3] For electronic materials, such as photogenerating pigments for photoconductors, the crystal packing may not only change the absorption spectrum but also modify the performance of the electronic device by affecting photogeneration efficiency and carrier mobilities.[4-7]

Crystallochromy,[8] that is the dependence of color on crystal packing, has been observed for a variety of pigment classes such squaraines,[9,10] phthalocyanines,[11] and other pigments such as 1,4-dithioketo-3,6-diphenylpyrrolo[3,4-*c*]pyrrole.[12] Given such a general pigment phenomenon, it would be of interest to understand the interrelationship between crystal packing and wavelength shift and ultimately to correlate the change in electronic structure with the photoconductive behavior of these pigments.

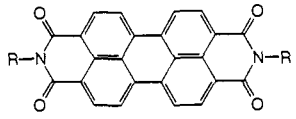

Compound No.	R Group	Color of Crystals
1	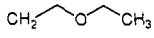	red
2	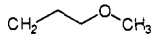	black
3	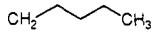	red
4	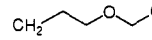	red
5	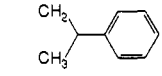	red
6	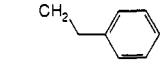	black
7	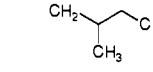	red
8	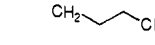	red-maroon
9		red
10	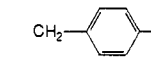	black
11	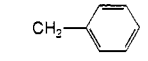	red-violet

Figure 1. Crystallochromy in perylene pigments.

Crystallochromy of Perylenes

Although the effect of packing on the color of pigments is a general phenomenon, perhaps its most marked manifestation is found in a remarkable series of compounds called perylenes, investigated by Graser and Hädicke and their collaborators at BASF.[8,13-15] Consider the 11 perylene derivatives shown in Figure 1. Although the basic chromophore for each pigment is identical,

† Xerox Research Centre of Canada.
‡ Cornell University.
• Abstract published in *Advance ACS Abstracts,* September 1, 1994.

(1) Venkataraman, K., Ed. *The Chemistry of Synthetic Dyes*; Academic Press: New York, 1970; Vol. 3.
(2) Griffiths, J. *Dyes Pigm.* **1982**, *3*, 211–233.
(3) Valdes-Aguilera, O.; Neckers, D. C. *Acc. Chem. Res.* **1989**, *22*, 171–177.

0002-7863/94/1516-9684$04.50/0

very small substituent changes on the periphery of the pigment chromophore lead to enormous changes in the color of these compounds. For example, moving the oxygen from position 3 in the side chain of 3-oxapentylperylene (**1**) to position 4 in 4-oxapentylperylene (**2**) transforms the color from red to black (the absorption maximum changes from 564 to 613 nm and the band broadens considerably[8,13]) in the solid state. Clearly, changes in these compounds are the manifestation of an aggregation effect since all of these materials have essentially the same absorption spectrum in solution.

A typical perylene structure is shown in **12**; others share the characteristics of this one, with important small differences. The first feature that one notices in the solid state is the stacking of the platelet-like molecules and then the offset of one plate from the next one in the one-dimensional chain. The stacking is universal (the perylene interplanar spacing, *d*, is near 3.5 Å for all planar perylene structures known).[16] The distance *d* is defined in structure **13**.

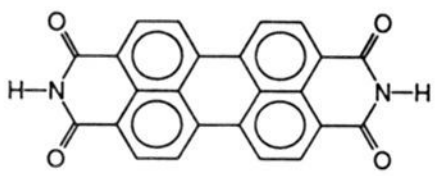

12

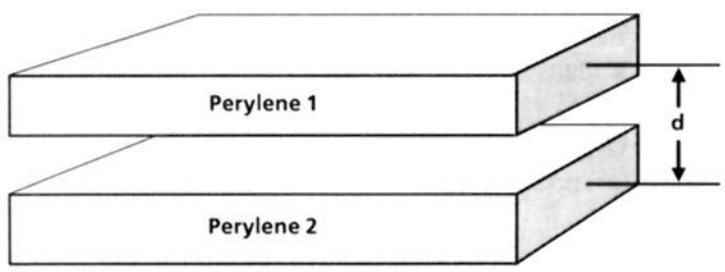

13

The offset differentiates one perylene from another. We define a transverse offset, *t*, and a longitudinal offset, *l*, as shown in **14**; *t* and *l* describe the coordinates of a given atom in the next perylene down the stack relative to the preceding one.

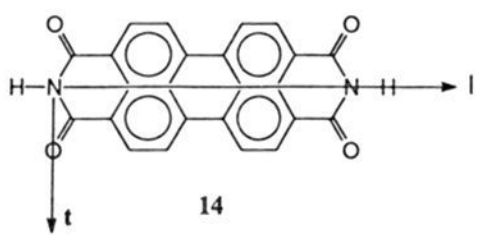

14

Klebe and his co-workers[8] were able to develop an empirical model which rationalized the visible absorption maxima for 24 perylene dyes in the solid state as a function of three crystal parameters, the perylene–perylene *d* spacing, *t*, the transverse offset, and *l*, the longitudinal offset. The wavelength λ_{max} is given by eq 1.

$$\lambda_{max} = 9.718t^2 - 82.009t - 21.888l + 735.329 \qquad (1)$$

Since most perylenes adopt in their crystal structures an interplanar *d* spacing of approximately 3.5 Å, *d* was not included in the empirical equation. The dependence of the absorption maximum in the solid state on the transverse and longitudinal offsets is shown in Figure 2. The longitudinal offset empirically causes a linear change in the wavelength, while the change in absorption maximum has a much steeper dependence on the transverse offset and falls off quadratically to 4 Å (the approximate width of the perylene molecule).

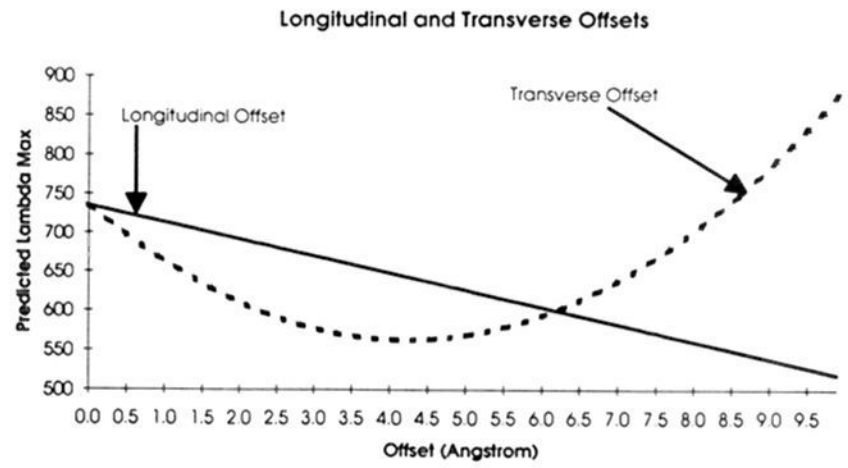

Figure 2. Empirical variation of the perylene absorption maximum with longitudinal and transverse changes according to eq 1.

This equation is empirical in nature and was not intended to explore the quantum-mechanical implications of the aggregation. Nevertheless, it serves as a convenient starting point for the discussion and as a reference point for contrasting the empirical behavior as a function of offset with what molecular orbital calculations predict.

Calculations

Our objective in this work is to develop a qualitative quantum-chemical understanding of the effects of aggregation, especially the stacking offset, on color in these dyes. In our analysis we use the extended Hückel semiempirical molecular orbital method. We will take advantage of the propensity of perylenes to stack in columns and so formulate the analysis as a one-dimensional problem. Although three-dimensional effects will, for some crystal motifs, serve to enhance the perylene–perylene interaction, the one-dimensional analysis was chosen for clarity of understanding. Also the size of the three-dimensional problem for a crystal structure based on a 40-atom molecule makes such a calculation prohibitive.

Calculations on dimeric and oligomeric systems were performed using the extended Hückel module in HyperChem on a Silicon Graphics 4D/480. In all cases standard parameters were used.[17]

The infinite, one-dimensional stack calculations were performed using the tight-binding method described previously.[18]

Ethylene

In order to facilitate the overall analysis, the simplest of all π systems, ethylene, was considered first. The ethylene analogy will allow us to interpret the band structure of the more complicated perylene example in the familiar context of molecular orbital theory.

The HOMO and LUMO of an isolated ethylene are shown in Figure 3. What happens if one examines not an isolated ethylene but a dimer, trimer, etc., derived from ethylene, its components

(4) Weigl, J. W.; Mammino, J.; Whittaker, G. L.; Radler, R. W.; Byrne, J. F. In *Current Problems in Electrography*; Berg, W. F., Hauffe, K., Eds.; Walter de Gruyter: New York, 1972; pp 287–300.
(5) Loutfy, R. O.; Hor, A. M.; Kazmaier, P.; Tam, M. *J. Imaging Sci.* **1989**, *33*, 151–159.
(6) McKerrow, A. J.; Buncel, E.; Kazmaier, P. M. *Can. J. Chem.* **1993**, *71*, 390–398.
(7) Kazmaier, P. M.; McKerrow, A. J.; Buncel, E. *J. Imaging Sci. Technol.* **1992**, *36*, 373–375.
(8) Klebe, G.; Graser, F.; Hädicke, E.; Berndt, J. *Acta Crystallogr.* **1989**, *B45*, 69–77.
(9) Buncel, E.; McKerrow, A.; Kazmaier, P. M. *J. Chem. Soc., Chem. Commun.* **1992**, 1242–1243.
(10) Loutfy, R. O.; Hsiao, C. K.; Kazmaier, P. M. *Photogr. Sci. Eng.* **1983**, *27*, 5–9.
(11) Wagner, H. J.; Loutfy, R. O.; Hsiao, Cheng-K. *J. Mater. Sci.* **1982**, *17*, 2781–2791.
(12) Mizuguchi, J.; Rochat, A. C. *J. Imaging Sci.* **1988**, *32*, 135–140.
(13) Graser, F.; Hädicke, E. *Liebigs Ann. Chem.* **1980**, 1994–2011.
(14) Hädicke, E.; Graser, F. *Acta Crystallogr.* **1986**, *C42*, 189–195.
(15) (a) Graser, F.; Hädicke, E. *Liebigs Ann. Chem.* **1984**, 483–494. (b) Hädicke, E.; Graser, F. *Acta Crystallogr.* **1986**, *C42*, 195–198.
(16) One of the perylene structures described in ref 8 with very bulky end groups (2,6-dimethylphenyl) has a perylene-perylene *d* spacing of approximately 7 Å.
(17) Hoffmann, R. *J. Chem. Phys.* **1963**, *39*, 1397–1412.
(18) Hoffmann, R. *Angew. Chem., Int. Ed. Engl.* **1987**, *26*, 846–878.

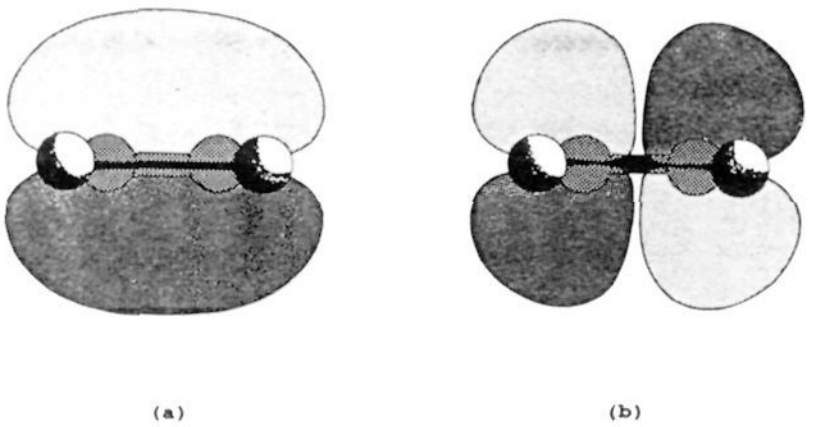

Figure 3. Isosurfaces, that is, surfaces of constant $\Psi = (x,y,z)$, of the ethylene HOMO (a) and LUMO (b) at 10% of the orbital maximum value d (light shading = positive and dark shading = negative phase of Ψ). The white spheres represent hydrogen atoms while the black spheres repesent carbons.

separated at the standard π molecular separation of 3.5 Å? Our chemical intuition can help us here. We know that at 3.5 Å the intermolecular interaction will be weak and that the molecular orbitals of the aggregate may be derived from the basic orbitals of the ethylene building blocks. Thus, for the dimer, the ethylene HOMO will give rise to two sibling orbitals, separated by a small energy difference. The new HOMO of the dimer, the less stable member of this set, is derived from the *antibonding* combination of the ethylene HOMO's, while the more stable sibling is derived from the bonding combination. A similar set can be derived from the parent LUMO's. The interaction diagram that shows these combinations is **15**.

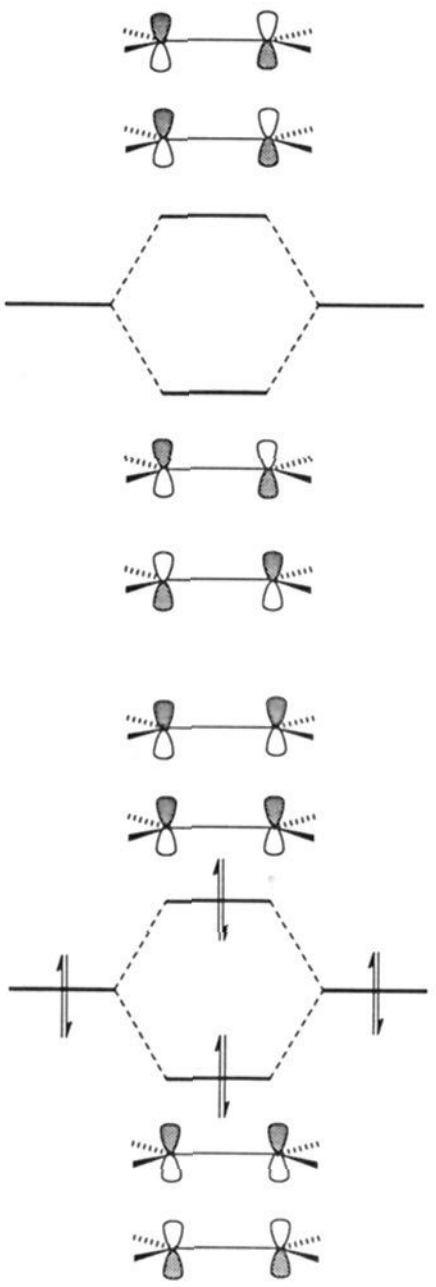

15

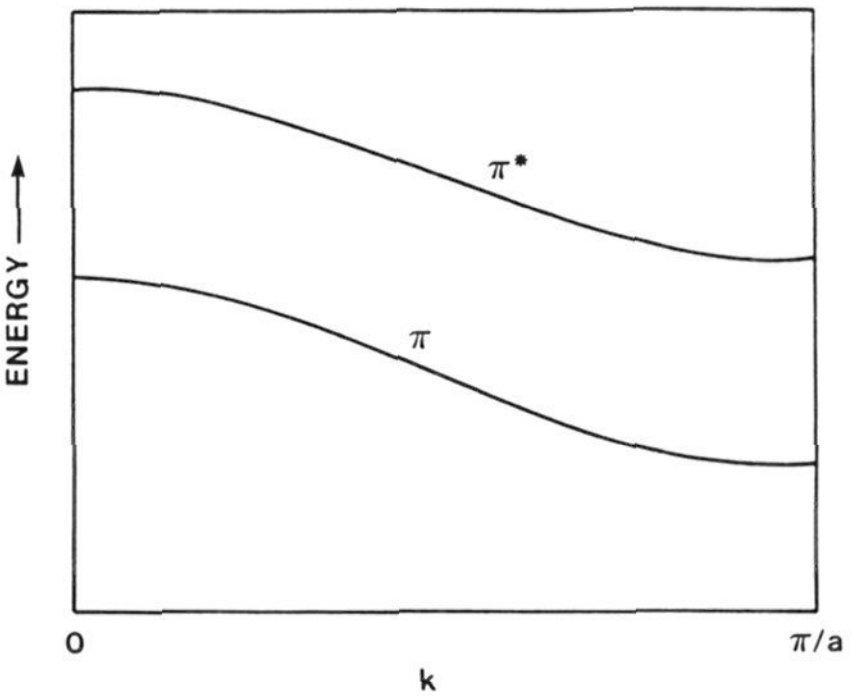

Figure 4. Variation of the energy levels within the π and π^* bands as a function of the wave vector k.

What happens if we extend this analysis to an eclipsed trimer, tetramer, pentamer, and ultimately an infinite one-dimensional stack? For the trimer, the HOMO gives rise to three sibling orbitals, the tetramer to four, and the pentamer to five.

The detailed orbital pattern is easily understood using a particle-in-a-box analysis.[19] The lowest orbital has all of the ethylene fragment molecular orbitals combining so that their overlap to all adjacent intermolecular orbitals is bonding. In contrast, the highest energy orbital consists of the combination of ethylene fragment MO's that gives the maximum number of nodes (four *intermolecular* nodes for the pentamer).

What does the electronic structure of a stack of many ethylenes (approaching infinity) look like? Each π and π^* level of the ethylene spreads out into a band.[20] The bottom of the band is the most bonding combination of the relevant orbitals, the top the most antibonding. The levels within a band are indexed by the wave vector k, with the range of k being between $k = \pi/a$ and $-\pi/a$. There is a double degeneracy at each k within the band, i.e. $E(k) = E(-k)$. The $k = 0$ combination of orbitals is $\chi_1 + \chi_2 + \chi_3 + \chi_4 + ...$, i.e. totally "in-phase"; $k = \pi/a$ is totally "out-of-phase", $\chi_1 - \chi_2 + \chi_3 - \chi_4 + ...$ Given the topology of π (or π^*) orbitals interacting, in each case, it is the $k = \pi/a$ combination which is the low-energy point, $k = 0$ being inter-ethylene antibonding.

The band structure is shown in Figure 4. Let us concentrate on the filled π band and see what happens if we slide the ethylenes past each other, first longitudinally. The deformation is defined in **16**.

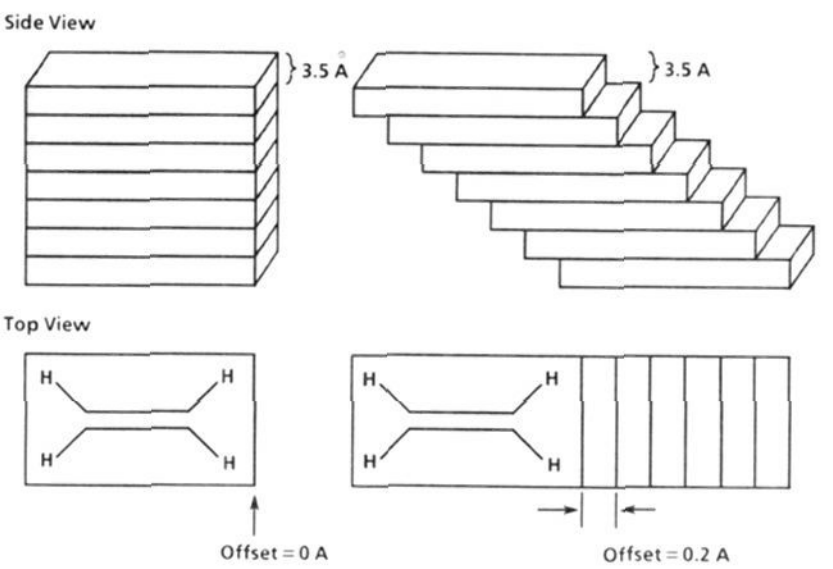

16

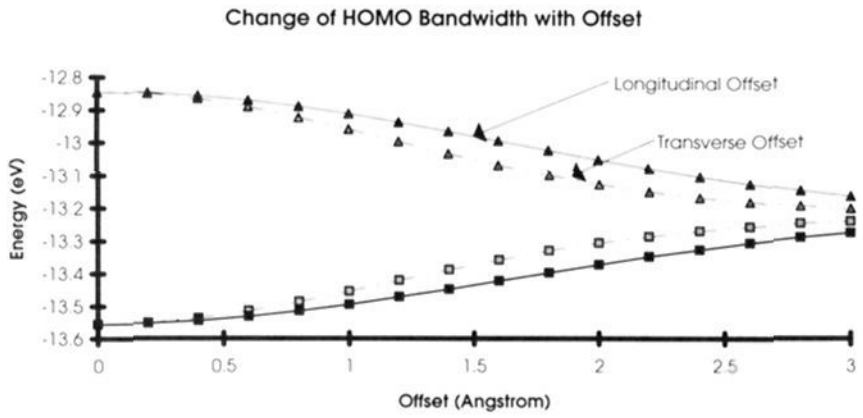

Figure 5. Change of the HOMO bandwidth with longitudinal and transverse offsets for the ethylene molecule.

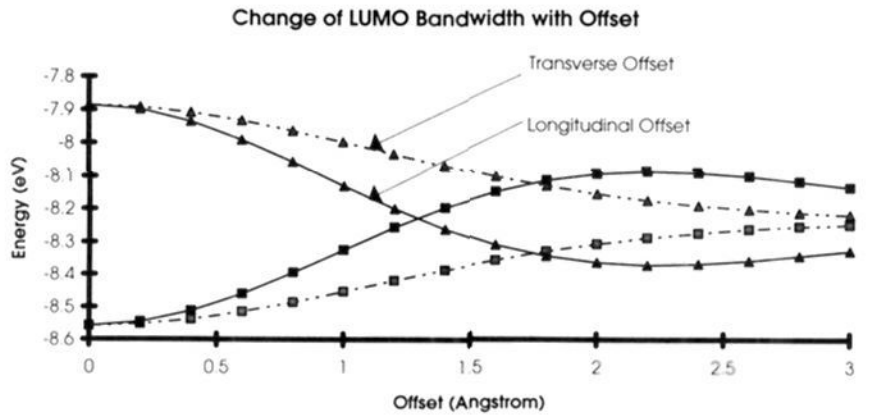

Figure 6. Change of the LUMO bandwidth with longitudinal and transverse offsets for the ethylene molecule.

Instead of the band structure, we plot just the top and the bottom of the filled π band in Figure 4. This is shown in Figure 5.

The longitudinal offset lowers the overlap between neighboring ethylene π orbitals as shown in **17**. Thus the bandwidth should decrease with the offset.

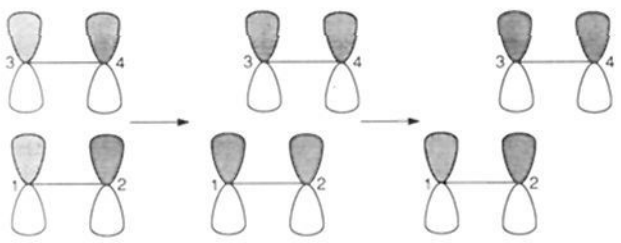

17

The transverse displacement for ethylene leads to a more rapid constriction of the bandwidth, very much as noted by Klebe et al.[8] in their analysis of the perylene system. This difference between longitudinal and transverse effects is a consequence of the geometry of the deformation. The overlap simply decreases more rapidly upon displacement in the transverse direction, as shown schematically in the "side-on" view, **18**.

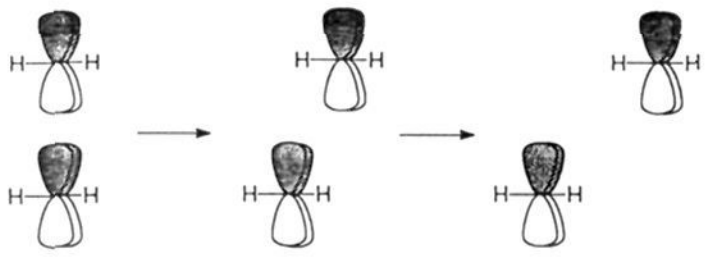

18

In contrast, the case for the π^* conduction band is quite different (Figure 6). While the transverse offset gives roughly the same monotonic decrease in the conduction bandwidth as we observed in the case of the valence band, the longitudinal offset leads to a rapid collapse of the bandwidth to zero (accidental complete degeneracy of all orbitals) and reemergence of the band with "inverted" orbital ordering, that is to say the crystal orbital at $k = 0$ is now most stable while the orbital at $k = \pi/a$ is least stable.

Why this difference? The effect of a transverse offset for the π^* orbital is pretty much the same as it is for π, as was shown in **18**. What happens for the longitudinal offset is quite different. As **19** shows for a representative in-phase π^* combination, the overlap in this orbital diminishes, due to increased 2–3 (orbital numbers in **19**) antibonding and decreased 1–3 bonding. If the offset is sufficient (**19**-c) the same k combination is net antibonding (see the 2–3 overlap). Somewhere between position c and the initial eclipsed position (a), the bonding and antibonding interactions cancel each other out and the bandwidth collapses to a single energy value (all the crystal orbitals in the band are degenerate).

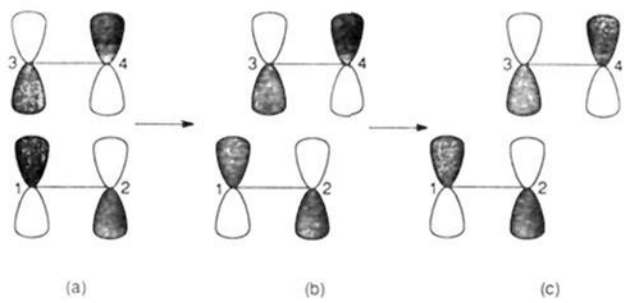

19

It is easy to generalize these conclusions for a stack of polyenes or other π systems. If one moves from ethylene to a diene, triene, etc., each orbital (except the lowest) has a certain number of longitudinal nodes. These are schematically indicated for the HOMO's and LUMO's of butadiene and hexatriene in **20**.

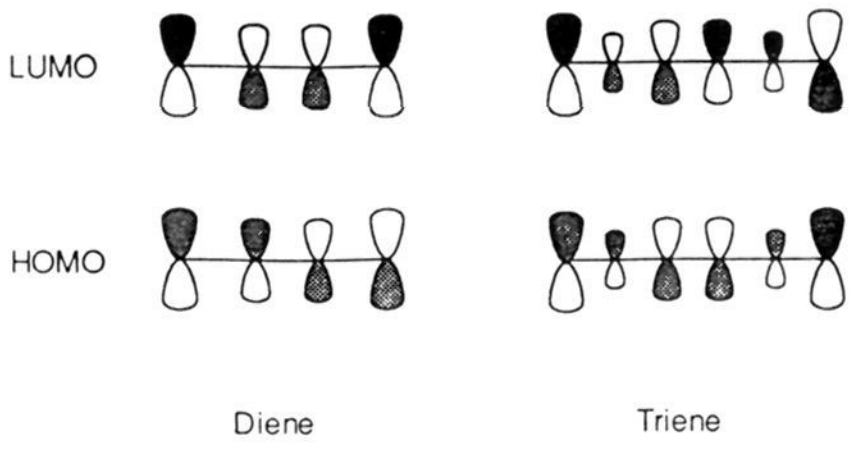

20

A transverse offset will in each case produce a simple diminution of the bandwidth of the bands derived from these MO's. A longitudinal offset will lead to oscillations in the bandwidth, the number of maxima depending on the nodal structure—two nodes for the HOMO of the diene, three for the LUMO of the diene and HOMO of the triene, and four for the LUMO of the triene.

The extrapolation to a flat π system that has a transverse "extent", as a perylene does, is pretty clear. The frontier orbital then may have transverse nodes as well as longitudinal ones, and there will be an oscillation in bandwidth for a transverse offset as well. To be specific (and general), if a given monomer MO has n longitudinal nodes and m transverse nodes, there should be in the bandwidth versus offset graph n and m points of zero bandwidth (not counting the point at infinite offset).

Another way of making a generalization is to observe that band broadening correlates with the area-of-overlap only if one

(19) Laidlaw, W. G. *Introduction to Quantum Concepts in Spectroscopy*; McGraw-Hill: New York, 1970; pp 23–26.
(20) Hoffmann, R. *Solids and Surfaces: A Chemist's View of Bonding in Extended Structures*; VCH: New York, 1988.

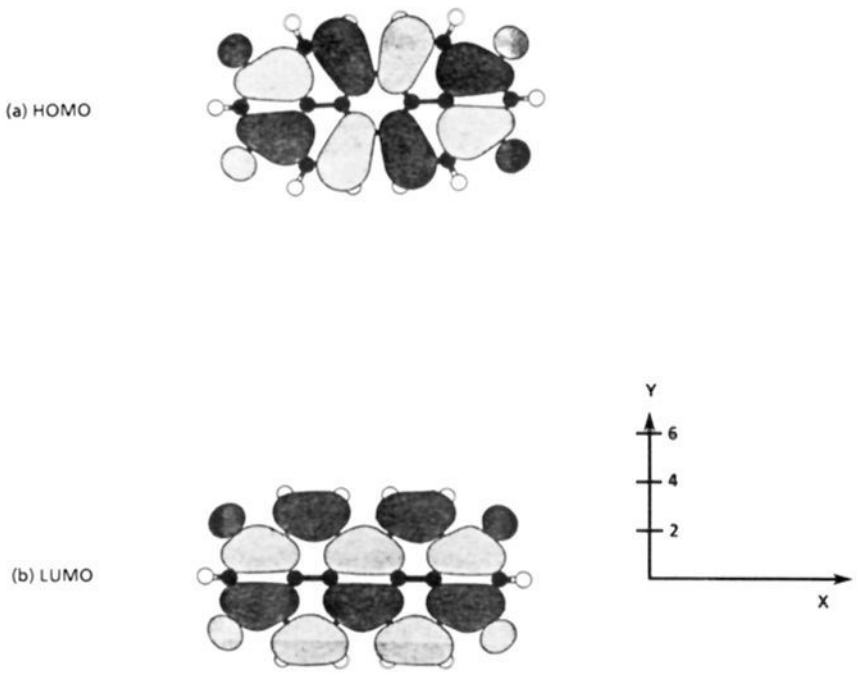

Figure 7. HOMO (a) and LUMO (b) orbitals for perylene imide (light shading = positive and dark shading = negative phase of the wave function).

selects *maxima in the oscillating bandwidth versus offset curve.* Node crossing, as was observed for the ethylene stack π^* conduction band on longitudinal offset, can lead to *narrow* bandwidths *even for large area overlaps.* Since an *increase* in the HOMO and LUMO bandwidth leads to a *decrease* of the band gap, the minimum π to π^* transition energy correlates with the area-of-overlap, as empirically observed by Klebe et al.,[8] *only if one selects maxima in the oscillating bandwidth versus offset curve.*

Having developed the analytical concepts for this simple system, let us now turn our attention to the more complicated perylene system.

Perylene Imides

The HOMO and LUMO for perylene imide **12** have the structures shown in Figure 7. Note three longitudinal and one transverse nodes in the HOMO (ignoring the node between the carbonyl oxygen and the framework) and three transverse nodes in the LUMO.

Suppose one were to eclipse an infinite stack of perylene imides, as shown in **21** at the left, and then gradually offset the two stacks in a longitudinal sense. The bandwidth as a function of the offset

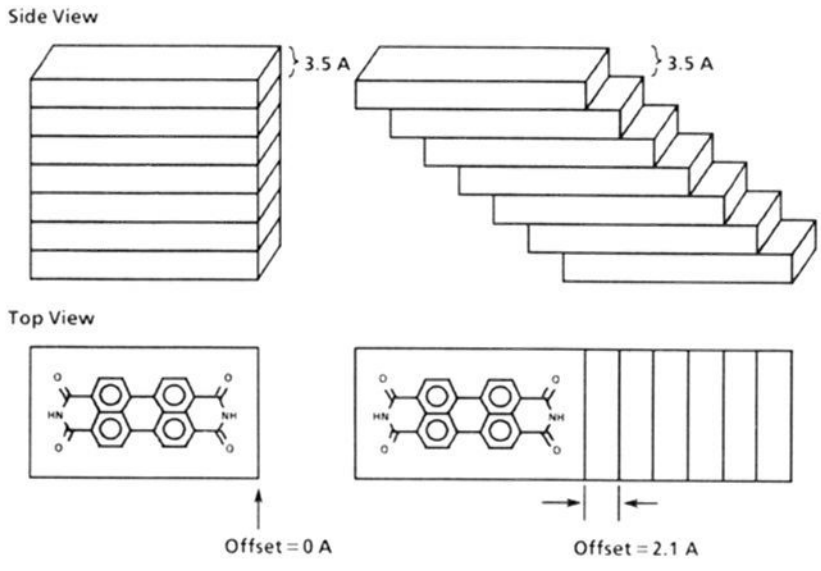

21

may be seen from a plot of the energy of the crystal orbitals with indices of $k = 0$ and $k = \pi/a$, the extrema of the crystal orbitals. The dependence of the bandwidth on the degree of longitudinal offset is shown in Figure 8.

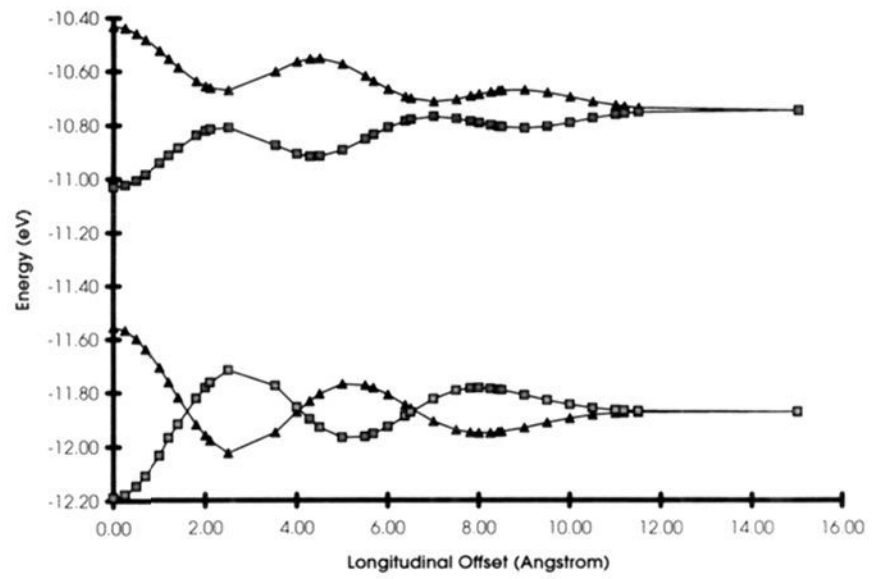

Figure 8. Variation of the valence and conduction bandwidths of perylene imide (**12**) as a function of the longitudinal offset.

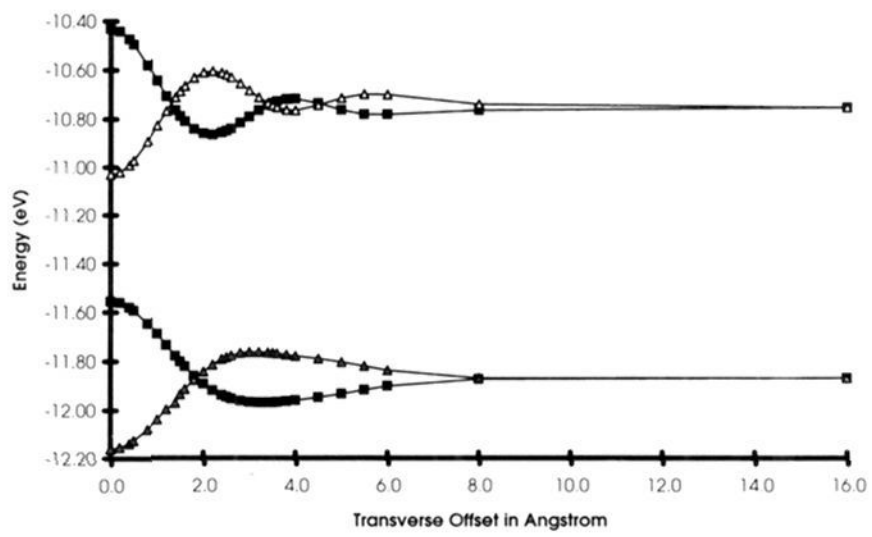

Figure 9. Variation of the valence and conduction bandwidths of perylene imide (**12**) as a function of the transverse offset.

The longitudinal and transverse offset behavior of the computed curves for the HOMO is consistent with our expectations—three transverse nodes and one longitudinal one leading to the same number of points of zero bandwidth. The three points of zero bandwidth in the transverse offset of the LUMO are similarly related to the three transverse nodes.

The longitudinal offset behavior of the conduction band is more complicated and merits discussion. There are three points of maximum bandwidth seen in Figure 8 (at 0, ≈4.0, and ≈8.5 Å offset), separated by two points of minimum, but not zero bandwidth (at ≈2.0 and ≈6.5 Å offset). Figure 8 shows that the LUMO has strictly speaking no longitudinal nodes. But things are not so simple, for there are no nodes in Ψ for some values of y (see the coordinate system in Figure 7) but there are nodes for others. For instance, for $y = \pm 1, \pm 3$ Å, there are no nodes as x is swept through, but for $y = \pm 2$ Å, there are six nodes. The wave function does not follow the rectangular restrictions of the x,y axes or the (transverse, longitudinal) description. It undulates.

To understand what happens, it is best to focus on whether the overlap is large or small along a distortion. For a longitudinal offset we start out with a large overlap between LUMO's for zero offset. Relative maxima will result when there is large overlap (good overlap of dark and light areas). This will take place for a shift by –4 and –8.5 Å. In between, there are regions of effective overlap as well as regions of minimal overlap (regions of positive overlap at one y canceling out regions of negative overlap at another y). These smaller overlaps will produce smaller bandwidths. But the bandwidth is never zero, because the controlling overlap is never zero by symmetry.

Figure 9 shows the corresponding influence of the transverse offset on the valence and conduction bandwidths. Once again, the nodal character of the HOMO and LUMO orbitals determines the oscillations in the bandwidth as the offset is increased from

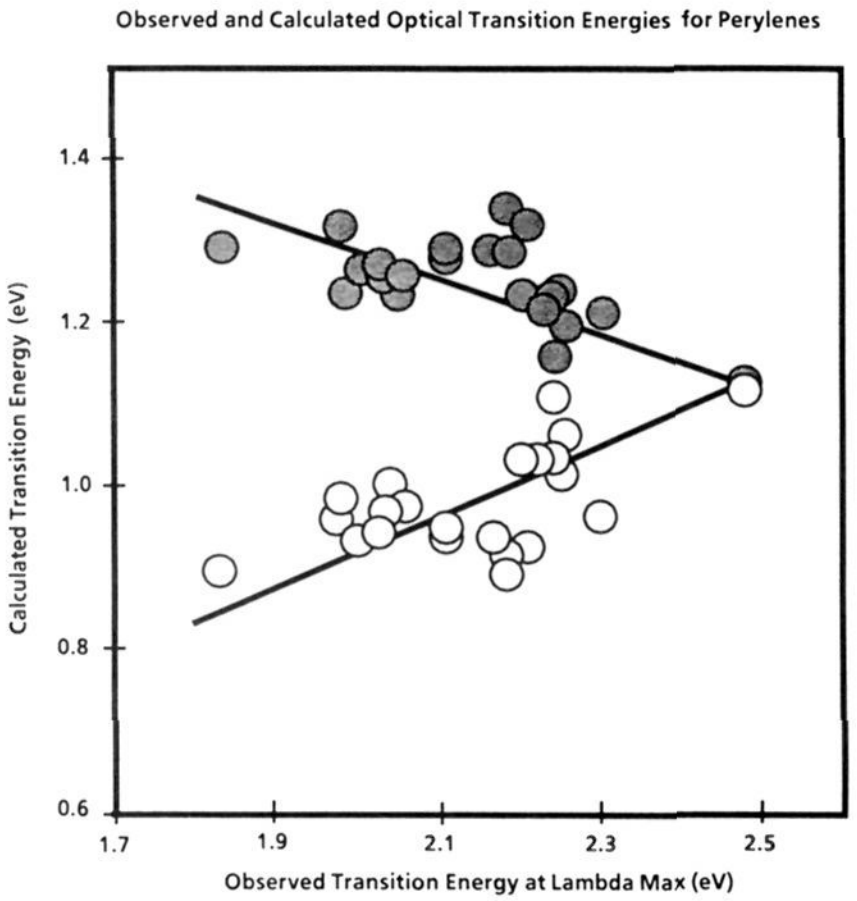

Figure 10. Observed and calculated transitions for perylene pigments. The open circles represent the band gap transition while the solid circles represent the transition from the bottom of the valence band to the top of the conduction band.

0 to 8 Å. There are less zones for the transverse offset bandwidths in the HOMO because there are less nodes to be swept by along the deformation.

In contrast to Graser and Hädicke's empirical results, in which the perylene structural data were fit to a function with a *linear*, *monotonic* decrease of wavelength with longitudinal offset, the molecular orbital analysis indicates that the nodal character of the HOMO wave function imposes conditions which lead to a catastrophic collapse of bandwidth for certain, specific offsets which give *very large area overlaps*. In order to determine whether or not the molecular orbital results are consistent with the observed absorption maxima reported for perylenes, it was of interest to calculate band gaps for perylenes with known longitudinal and transverse offsets. Klebe et al.[8] report sets of interperylene *d* spacings, longitudinal and transverse offsets for all of the compounds used in the generation of the empirical correlation reported in their paper. However, the property of crystallochromy is manifested not only in the shift of the absorption maximum but also in a general broadening of the absorption.[13] For that reason, extended Hückel calculations were performed at the offsets and *d* spacings described.[8] Both the calculated band gap and the maximum energy valence-conduction band transitions were plotted as a function of the experimental absorption maxima. These results are shown in Figure 10.

The calculated results correlate reasonably linearly with the experimental results. Not only does the band gap correlate with energy of absorption but the broadness of the absorption qualitatively correlates with the band broadening. It is not surprising that the extended Hückel method underestimates the overall energy of the transition since the propensity for extended Hückel method to give too small band gaps is well-known.[21,22] The current theoretical estimates for the band gap in perylenes, 48–49% of the observed values, are similar to those values for the underestimation of the conducting polymer benzimidazobenzophenanthroline (BBL) reported by Hong et al.[22]

Relationship of Band Broadening to Photoconductivity and Conductivity in Organic Crystals

The offset of the perylene crystal packing is reminiscent of the stacking behavior of organic conducting crystals such as tetrathiafulvalene–tetracyanoquinodimethane (TTF–TCNQ). These compounds crystallize in such a way that the TTF and TCNQ components form separate stacks within the crystal. Lowe[23] and Silverman[24] have discussed the origin of the slipped stack effect in the TTF–TCNQ system. Lowe,[23] in his analysis of the electronic structure of these crystal aggregates, observed that, for the neutral system (that is, the case where no charge was transferred from the TTF stacks to the TCNQ stacks), the dominant interaction was a four-electron repulsion in both stacks. If however one electron is transferred from every second TTF unit to every second TCNQ unit, then within each stack the four-electron repulsion is replaced by a three-electron and/or one-electron interaction as the predominant *intermolecular* interaction. Thus, by choosing the appropriate electron donor to give up the electron and an excellent electron acceptor to receive an electron, the overall energetics for this process become favorable. One can then explain the net transfer of charge which is observed experimentally and which leads to the conductivity of these systems, since the bands in the solid state are now partially filled.

In the case of a photoconductor such as a perylene, one does not have two entities with different charge donation and charge acceptance propensities as in the TTF–TCNQ system, and so, one cannot expect a transfer of charge in the ground state. However, this is not true of the excited state for these compounds. For example, it has been noted on several occasions[25,26] that charge-generating pigments almost invariably contain both donor and acceptor moieties in the same molecule. If an electron were formally transferred from the HOMO of one perylene to the LUMO of a nearby perylene in a one-dimensional stack as shown in **21**, then the simple four-electron intermolecular repulsion interaction present in the ground state would be alleviated and replaced by one- and three-electron intermolecular interactions. These stabilizing interactions would affect the system maximally when the four-electron destabilization is most severe, i.e. when molecule–molecule HOMO–HOMO overlap is at a maximum (when the valence band is most broad), and minimally when the HOMO–HOMO overlap is negligible.

But how does this observation affect photoconductivity and, in particular, charge generation in organic pigments? The charge generation process is discussed in terms of two general mechanisms, the Onsager process[27–29] and the exciton migration mechanism.[30] A factor in the Onsager mechanism for charge generation is the recombination rate. The favorable interaction observed on excitation of pigments with substantial band broadening would stabilize the separated charge and inhibit recombination. Similarly, in the exciton migration mechanism, the exciton must survive annihilation long enough to migrate to the pigment particle surface in order to allow the formation of separated holes and electrons by the sensitizer. Stabilization of the exciton would lead to an increase in exciton lifetime and thus allow more diffusion to the interface.

In summary, we predict that pigments within a series with the molecular morphology of the perylenes (clearly defined longitudinal and transverse axes) would show higher photosensititivies when there is substantial valence and conduction band broadening

(21) Whangbo, M.-H.; Hoffmann, R.; Woodward, R. B. *Proc. R. Soc. London, Ser. A.* **1979**, *366*, 23–46.
(22) Hong, S. Y.; Kertesz, M.; Lee, Y. S.; Kim, Oh-K. *Macromolecules* **1992**, *25*, 5424–5429.
(23) Lowe, J. P. *J. Am. Chem. Soc.* **1980**, *102*, 1262–1269.
(24) Silverman, B. D. In *Crystal Cohesion and Conformational Energies*; Metzger, R. M., Ed.; Topics in Current Physics, Vol. 26; Springer: Berlin, 1982; pp 108–136.
(25) Law, Kock-Y. *Chem. Rev.* **1993**, *93*, 449–486.
(26) Perlstein, J. H. Polymers in Electronic Applications. Ninth Annual Summer Institute in Polymer Science and Technology, June 11, 1979. Perlstein, J. H. Structure and Charge Generation in Low-Dimensional Organic Self-Assemblies. In Electrical Properties of Polymers; Diamond, A. S., Ed.; Academic Press: New York, 1982; pp 59–91.
(27) Pai, D. M.; Melnyk, A. R. in *Proceedings of SPIE—The International Optical Engineering*; SPIE: Bellingham, WA, 1986; Vol. 617, pp 82–94.

manifested as red shifts on aggregation. It is precisely in the band broadened crystal motifs where the four-electron destabilization is most severe and where charge separation on excitation can be most beneficial.

Before citing examples of pigment classes which exhibit this behavior, it is essential to point out some caveats to this analysis. First of all it is important to compare single wavelength photosensitivities. Since the aggregation process may dramatically change the absorption spectrum of the photoconductor, one needs to be sure that the increased photosensitivity is not simply due to an increase in the number of photons absorbed because of the broadened wavelength response of the pigment. Secondly, the significant parameter is the change in bandwidth as a function of aggregation. If one compares two chromophores where the solution and/or gas-phase spectra are different, one needs to relate the bandwidth change to the unaggregated pigment using this absorption wavelength as a reference.

For perylenes, it has been known for some time that structural features which inhibit close interaction in the solid state also lead to low generation efficiencies.[5,31] Indeed, structures which allow for very little band broadening, such as compound **22**, have negligible photogenerating efficiencies.

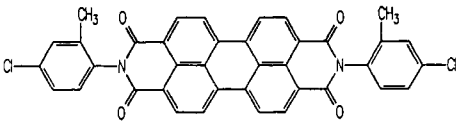

22

Phenethylperylene (**6**) also should show marked band broadening in the solid state as indicated by the current calculations. The photoconductivity of this material ($E_{1/2}$), that is, the light energy required to discharge the device to one-half of its initial potential in a multilayer device, is reported[32] to be 2.4–2.6 erg/cm^2. In the perylene series, compounds which exhibit the largest band broadenings are also those with the higher photosensitivities. Are these general principles born out in the major pigment classes where photogeneration is observed?

Squaraines are another class of photogenerating pigments with rodlike molecular morphologies. They also possess the donor–acceptor architecture common to most photogenerator pigments. Structure–activity relationships have shown that a planar geometry is consistent with high photogenerating efficiencies if the packing leads to substantial broadening of the absorption in the solid state.[10] Indeed, in this series of compounds studied, as shown in Figure 11, all highly photoactive materials showed substantial absorption broadening in the solid state and the degree of exciton splitting could be correlated to the photosensitivity of the pigment in question.

Thiopyrylium dyes, particularly compound **23**, in their unaggregated state show low sensitivity. Aggregation results in a

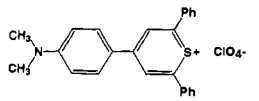

23

shift in the absorption maximum from 580 to 680 nm (Figure 12) with a 100-fold increase in xerographic sensitivitites. More pertinent to the present discussion is the observation that the skewed absorption peak has broadened considerably. Thus high photosensitivities are reported under those circumstances which

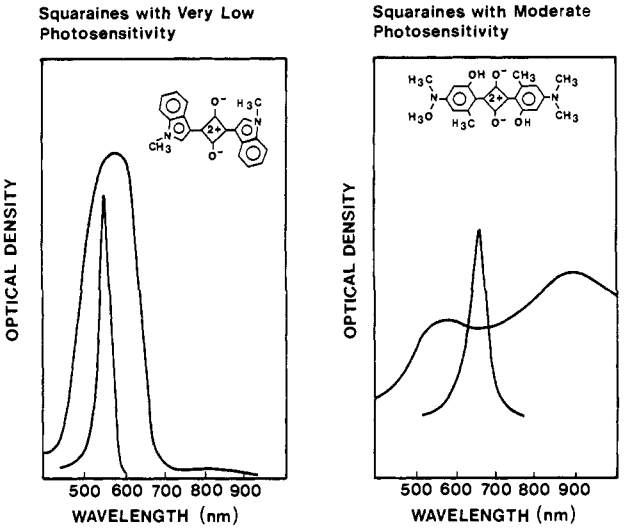

Figure 11. Plots showing that squaraines with high photosensitivities show very broad visible absorptions in the solid state when compared to squaraines of low photosensitivities. The sharp peaks are solution absorption spectra in methylene chloride while the broad peaks represent the solid-state absorption. Reprinted with permission from ref 10. Copyright 1983 The Society for Imaging Science and Technology.

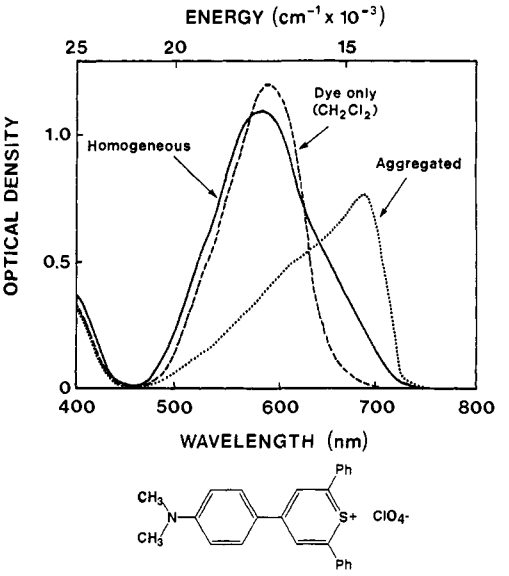

Figure 12. Aggregation and comcomitant broadening of the absorption spectra of thiopyrylium dyes occurs in concert with a 100-fold increase in photosensitivity. Reprinted with permission from ref 34. Copyright 1978 American Institute of Physics.

show a substantial red shift coupled with substantial band broadening on aggregation.[26,33,34]

Finally, diketopyrroles, particularly compound **24**, have recently been described as a new class of photogenerator materials. Once

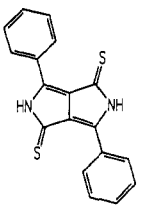

24

again the compounds undergo a red shift on solvent exposure[12] (Figure 13), and it is the substantially band-broadened aggregate which shows very high photosensitivity.

(28) Onsager, L. *Phys. Rev.* **1938**, *54*, 554–557.
(29) Onsager, L. *J. Chem. Phys.* **1934**, *2*, 599–615.
(30) Popovic, Z. D.; Hor, Ah-M.; Loutfy, R. O. *Chem. Phys.* **1988**, *127*, 451–457.
(31) Loutfy, R. O.; Hor, A. M.; Kazmaier, P. *Front. Macromol. Sci.* **1989**, 437–442.

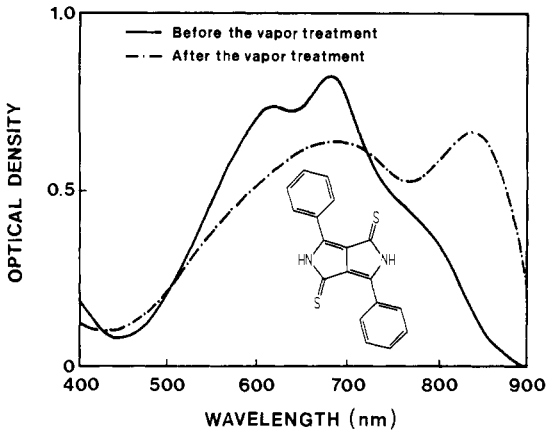

Figure 13. Plot showing that solvent vapor treatment of a diketopyrrole photoconductor leads to a broadening of the solid-state absorption spectrum and a marked increase in photosensitivity. Reprinted with permission from ref 12. Copyright 1988 The Society for Imaging Science and Technology.

Phthalocyanines and azo compounds represent two other pigment classes which contain highly photosensitive materials. The C_{4v} symmetry normally associated with phthalocyanines is radically different from the perylene pigments investigated here, so a discussion of phthalocyanines will have to await a detailed analysis of that chromophore. Azo compounds, on the other hand, are very unusual in that several *noncrystalline* photogenerator pigments have been reported. That observation suggests that azo pigments are unique as photogenerators and do not behave as other classes of photogenerator pigments.

Conclusions

Tight-binding extended Hückel calculations on infinite one-dimensional stacks of perylene pigments have shown that the bandwidth of the valence and conduction bands is determined not only by the degree of overlap between adjacent perylene moieties in the stack but also by the nodal characteristics of the HOMO and LUMO orbitals of the individual perylenes. Thus, some intermolecular orientations with very large area overlaps between adjacent perylenes may have very small valence and/or conduction bandwidths if the primary intermolecular overlap vanishes. This is a quantum-mechanical interference effect.

Comparison of the calculated band gaps to the energies of the absorption maxima for a series of perylenes for which the crystal structures are known indicates that the calculations can simulate both the trend in the wavelength maximum and the broadening of the absorption as a function of the one-dimensional geometry, even though three-dimensional interactions have been omitted.

These calculations also indicate that the donor–acceptor structure of photogenerating pigments is important, since stabilization of the hole–electron pair occurs by a mechanism which replaces the electron repulsion in the ground state with three- and one-electron interactions in the crystal excited state.

Within pigment series such as perylenes, squaraines, thiopyryliums, and diketopyrroles, compounds which exhibit the maximum band broadening on aggregation are predicted to have the longest hole–electron/exciton lifetimes and lead to the highest photosensitivities. The details of the stabilization of the hole–electron pairs in photogenerator pigments of phthalocyanines will be the subject of additional investigation.

Acknowledgment. Special thanks are due to Dr. Greg Zack and the members of the Xerox Design Research Institute at the Cornell Theory Center for their hospitality. The authors would like to thank Dr. John Shaw for programming assistance in adapting the extended Hückel program for plotting on the Sun workstation.

(32) Borsenberger, P. M.; Regan, M. T.; Staudenmayer, W. J. Multi-Active Photoconductive Insulating Elements Exhibiting Very High Electrophotographic Speed and Panchromatic Sensitivity and Method for their Manufacture. U.S. Patent No. 4,618,560.

(33) Borsenberger, P. M.; Chowdry, A.; Hoesterey, D. C.; Mey, W. *J. Appl. Phys.* **1978**, *49*, 5555–5564.

(34) Dulmage, W. J.; Light, W. A.; Marino, S. J.; Salzberg, C. D.; Smith, D. L.; Staudenmayer, W. J. *J. Appl. Phys.* **1978**, *49*, 5543–5554.